International Journal of Transport Development and Integration
https://www.acadlore.com/journals/IJTDI

Optimizing Artificial Neural Networks Modelling in Predicting International Roughness Index for Flexible Pavement

Lendra[1*], Mochamad Agung Wibowo[2,3], Jati Utomo Dwi Hatmoko[3]

[1] Department of Civil Engineering, Palangka Raya University, 73112 Palangka Raya, Indonesia
[2] Doctoral Program of Information System, Postgraduate School, Diponegoro University, 50241 Semarang, Indonesia
[3] Department of Civil Engineering, Diponegoro University, 50241 Semarang, Indonesia

* Correspondence: Lendra (lendraleman@jts.upr.ac.id)

Received: 09-20-2025 **Revised:** 12-25-2025 **Accepted:** 12-27-2025

Citation: Lendra, M. A. Wibowo, and J. U. D. Hatmoko, "Optimizing artificial neural networks modelling in predicting international roughness index for flexible pavement," *Int. J. Transp. Dev. Integr.*, vol. 10, no. 1, pp. 45–63, 2026. https://doi.org/10.56578/ijtdi100104.

Abstract: Accurate road roughness prediction is essential for sustainable transportation planning and cost-effective maintenance strategies. This study develops a systematic algorithm to optimize Artificial Neural Networks (ANN) for predicting International Roughness Index (IRI) values using Equivalent Standard Axle (ESA) and road age as primary inputs. The methodology employs comprehensive parameter space exploration across four optimization stages, evaluating various ANN configurations to identify the most effective architecture. Rigorous statistical validation through Analysis of Variance (ANOVA) and cross-validation ensures model reliability. Data quality assessment with outlier detection using the Interquartile Range method was implemented, retaining 94.3% of original observations. The optimized 6-30-25-20-1 ANN configuration, employing logsig and purelin transfer functions, achieved strong performance metrics, including R = 0.9554, R^2 = 0.9020, MSE = 0.0153, RMSE = 0.1236, and MAPE = 0.0285. Statistical validation confirmed significant model improvements with an F-statistic of 24.367 and a cross-validation mean of 0.892. The RMSE accuracy of 0.1236 m/km enables reliable pavement condition classification within established IRI thresholds, supporting timely maintenance decisions. This streamlined approach addresses critical infrastructure management challenges by enabling cost-effective maintenance planning with minimal data requirements, particularly valuable for developing countries with limited pavement monitoring infrastructure. The model's computational efficiency facilitates network-wide deployment for long-term planning and strategic resource allocation. Road agencies can apply this model for maintenance budget prioritization, network-level condition assessment, and multi-year intervention scheduling, particularly in resource-constrained environments where comprehensive pavement monitoring systems are unavailable. This study establishes a structured approach to optimize ANN for IRI prediction, enhance the effectiveness of Pavement Management Systems (PMS), and support sustainable transportation infrastructure through improved maintenance scheduling.

Keywords: Artificial neural network, Construction management, International roughness index, Machine learning, Road maintenance

1 Introduction

Road pavements deteriorate in condition, bearing capacity, and serviceability with age, traffic volume, and the influence of several elements such as pavement type and environmental conditions [1–4]. Structural and functional deterioration leads to reduced pavement serviceability [5, 6]. The smoothness of the road surface impacts driving safety, performance, and comfort [7–9]. In modern technology, infrastructure maintenance is one of the most important aspects of maintaining highway performance and safety [10]. A key maintenance component is determining the optimal maintenance time, which requires precise forecasting of road conditions [11]. International Roughness Index (IRI) measurements have become a widely used criterion for assessing road surface quality in this context, as they can help control and manage roadway conditions [12, 13]. By identifying the optimal time to perform maintenance, IRI forecasting can help highway management reduce losses caused by poor road quality [14].

Road repair is required when pavement condition becomes rough enough to compromise the safety and comfort of users [15, 16]. The condition of the pavement has a significant impact on the accident rate. The condition of the

pavement significantly impacts the accident rate. Therefore, pavement condition should be considered when planning maintenance, rehabilitation, and reconstruction [17]. Road surface roughness is quantified by IRI [11, 18–20]. Road authorities use Intelligent Transportation Infrastructure (ITI), a system developed by the World Bank and introduced by the National Cooperative Highway Research Program (NCHRP) in the 1980s [21]. IRI values indicate pavement unevenness and support more efficient maintenance planning [22, 23]. Accurate road roughness prediction is necessary for sustainable transportation, enabling planners to develop cost-effective maintenance and rehabilitation strategies [22]. Pavement surface roughness is influenced by many factors, including traffic volume, weather, pavement composition and structural design, construction quality, and continuous maintenance and rehabilitation activities [24]. Pavement performance models, also called deterioration or evolution models, should be integrated into Pavement Management Systems (PMS). Based on thorough data analysis, these models are used to forecast future pavement conditions [25]. Road Maintenance and Rehabilitation (M&R) can use limited resources most effectively by strategically planning and coordinating treatment activities based on pavement performance forecasts for the upcoming years [11].

Many prediction models are now used, ranging from conventional linear and non-linear regression models to advanced machine learning techniques such as Artificial Neural Networks (ANN) and Gene Expression Programming [26]. Notably, ANN has gained traction as a modelling technique in various pavement applications. Unfortunately, few studies have described how to build the algorithm and which functions are included, so that it can produce the best model for predicting IRI. For instance, researchers have used ANN to develop models for IRI prediction in rigid pavements [25], and for predicting subgrade elastic modulus [27–29]. Additionally, ANN has been applied in numerous studies for diverse purposes, including asphalt dynamic modulus prediction [30, 31], correlating pavement roughness with structural performance [32], and selecting pavement maintenance strategies while recalculating pavement layer properties [31, 33–35].

ANN-based IRI prediction models have gained popularity in recent years. However, a notable research gap exists in systematic approaches to parameter optimization. Most existing studies lack structured methodologies for parameter tuning, which is necessary for developing accurate predictive models [36, 37]. Finding optimal ANN parameters remains challenging, as no standardized approach to parameter selection has been established [38]. This gap is particularly evident in road maintenance prediction, where precise modeling can yield considerable cost savings and improved infrastructure management. A systematic trial-and-error method for ANN parameter optimization is therefore needed. Previous studies have demonstrated the effectiveness of trial-and-error approaches [39]. To address these limitations and contribute to the field, this study develops an ANN model to forecast IRI values using traffic load such as Equivalent Single Axle Load (ESA) and road age through a systematic optimization algorithm. This algorithm can be used in future research to test and evaluate IRI prediction models for both flexible and rigid pavements on toll roads.

Recent advances in neural network optimization have introduced sophisticated techniques, including Transformer-based architectures and Bayesian optimization methods [40]. Studies by Zhang et al. [41] demonstrated that hybrid optimization approaches can improve convergence speed by up to 40% compared to traditional methods. However, these advanced techniques often require substantial computational resources and specialized expertise, which may limit their applicability in practical pavement management scenarios, particularly in developing countries [42, 43].

This study addresses the identified research gaps by making the following key contributions to pavement management practice:

• A systematic parameter optimization framework: A four-stage trial-and-error methodology for ANN architecture selection that provides comprehensive parameter space exploration, offering a replicable approach where standardized methods are currently lacking in IRI prediction modeling.

• Minimal-data prediction capability: Development of an IRI prediction model using only ESA and road age as inputs, eliminating the need for extensive historical pavement condition data, and enabling deployment in regions with limited monitoring infrastructure.

• Practical validation for toll road networks: Rigorous statistical validation through Analysis of Variance (ANOVA) and cross-validation, demonstrating model applicability for flexible pavements on toll roads, with computational efficiency suitable for network-level implementation in resource-constrained settings.

These contributions provide road agencies with an accessible yet accurate tool for maintenance prioritization and budget allocation, particularly valuable for developing countries seeking cost-effective pavement management solutions.

2 Material and Methods

2.1 Artificial Neural Networks

The ANN debuted in the early 1950s, originating from psychologist Donald Hebb, who delved into the neural mechanisms of learning in the brain, culminating in the formulation of Hebb's Law [44]. As a subset of machine learning techniques, ANN derives inspiration from neurobiological principles, thereby emulating cerebral

functionality [45, 46]. Rosenblatt further elucidated this concept by introducing the perceptron training algorithm, marking the inception of a mathematically viable model amenable to computational simulation [47]. The advent of the backpropagation training algorithm in 1980 gave engineers a compelling impetus to explore ANN as a rapid and simple resource for mathematical modelling [48, 49]. Demonstrating adeptness in handling complex datasets exhibiting non-linear tendencies and lacking adherence to conventional mathematical frameworks, ANN furnishes a notably accurate solution for empirical modelling endeavours [50]. Reflecting neurological processes, ANN shows an architectural assembly of the human brain marked by a significant degree of parallelism [51].

ANN excel in handling applications marked by complex multi-parameter interactions [52, 53]. ANNs have demonstrated their efficacy in approximating complex nonlinear functions using input-output data [54]. The approximation prowess inherent in this soft computing paradigm is the primary impetus, as delineated by Eq. (1) herein [4]. Eq. (1) is met for any vector-valued continuous function $\mathrm{g(x)}$ defined on a subset $\mathrm{A} \subset \mathrm{Rn}$ where $\mathrm{x} \in \mathrm{A}$ and any $\in > 0$. There is a function $f(x)$ associated with x.

$$\sup_{x \in A} \|g(x) - f(x)\| < \epsilon \tag{1}$$

The Equation is a clear testament to the prowess of ANN in approximating non-linear functions. For example, neural network-based modelling provides a natural way to forecast IRI values for rigid pavements by leveraging unpredictable climate and traffic information commonly provided by regional state agencies such as the Department of Transportation (DOT) [4]. Generally, an ANN comprises an input layer, an output layer, and a series of hidden layers [55], where intricate non-linear computations occur, as depicted in Figure 1.

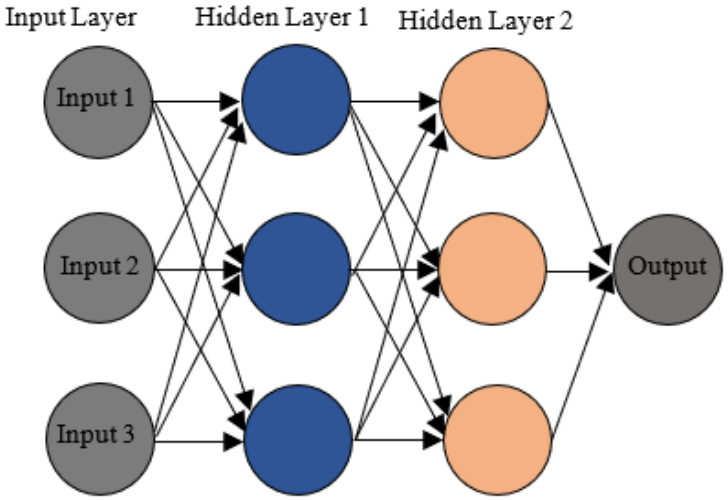

Figure 1. General architecture of the artificial neural networks [56]

Three basic components make up an ANN: (1) input neurons, also referred to as processing elements, which process inputs like traffic and climate data along with other parameters; (2) connection weights, which create connections between inputs and outputs; and (3) output neurons, which represent IRI values. ANN is based on a computational intelligence paradigm that emulates the functioning of biological nervous systems.

ANNs comprise a variable number of layers, depending on data complexity and network architecture. Multi-layer configurations may include more than one intermediary layer, commonly called hidden layers, which enhance training by adjusting the connecting weights to yield optimal models [57]. Each layer comprises a cluster of neurons interconnected via synapses. These synapses, representing connections, initially have weights that are modified during the iterative network operation. The standard approach for most neural networks begins with the training phase, followed by cross-validation and testing, during which predicted outputs are compared with actual outputs. Given ANN's ability to handle data devoid of conventional mathematical relationships, the resulting solution is often considered a black box [58].

The efficacy of the entire mechanism primarily hinges on the arrangement of neuron connections, the methodology employed for determining connection weights (termed the learning algorithm), and the neuron activation function (also known as the transfer function) [59]. Discrepancies in architectural comprehension arise across various studies, yielding divergent outcomes. Broadly, several ANN parameters, including the number of hidden nodes and layers, necessitate meticulous adjustment during training, as these configurations significantly impact model accuracy. Typically, trial-and-error methodologies are employed to ascertain optimal parameter settings [60]. Consequently, the trial-and-error approach will be employed in this investigation to discern the most effective model.

2.2 Parameter Selection Justification

The selection of ESA and road age as primary input parameters is strategically based on several practical and theoretical considerations. Traffic loading is universally recognized as the dominant factor influencing pavement deterioration, with numerous studies demonstrating its critical role in structural and functional degradation [2, 61]. Researches by Elhadidy et al. [62] and Santos et al. [63] in genetic algorithm-based pavement optimization confirmed that traffic parameters consistently emerge as the most significant predictors in pavement performance models. Road age represents the cumulative effects of time-dependent deterioration processes, including environmental factors, material aging, and repeated loading cycles [6, 64].

While comprehensive pavement condition assessments incorporating multiple distress indicators (cracking, rutting, surface defects) can enhance prediction accuracy [7, 65], such detailed data collection requires specialized equipment and substantial resources. Studies in metropolitan areas have demonstrated that simplified models using primary indicators can achieve acceptable accuracy for maintenance planning while remaining cost-effective [18, 66]. This streamlined approach is particularly advantageous for developing countries, where extensive pavement condition-monitoring infrastructure may be limited [11].

The decision to focus on these two parameters aligns with data availability constraints in Indonesian toll road systems, where traffic monitoring is systematically conducted but detailed distress surveys are performed less frequently. This approach ensures model applicability across the national toll road network while maintaining practical implementation feasibility for routine maintenance planning.

Environmental factors such as temperature variation, rainfall intensity, and freeze-thaw cycles undoubtedly influence pavement deterioration rates. However, incorporating these parameters would require: (1) extensive historical climate data collection at multiple locations, (2) complex data preprocessing and synchronization procedures, and (3) significantly increased model complexity. While acknowledging this as a limitation, the current model prioritizes practical implementability and data availability.

2.3 Method of Building Artificial Neural Network Model for Predicting International Roughness Index Value

2.3.1 Input node

There are two types of input nodes, namely ESA and road age, with the following conditions.

i. Traffic Load (ESA).

The data collected are traffic volumes per class per year, based on the classification of vehicles as defined in the Republic of Indonesia's Decree of the Minister of Public Works, number 370/KPTS/M/2007, dated August 31, 2007 [67], as shown in Table 1 below. Furthermore, the traffic volume is converted into traffic load to standard load or ESA by using the Equivalent Load Factor or Vehicle Damage Factor (VDF), with the following Eq. (2):

$$\mathrm{ESA_{I-V}} = \mathrm{VL_{I-V}} \times \mathrm{VDF} \times \mathrm{DD} \times \mathrm{DL} \tag{2}$$

where,

$\mathrm{ESA_{I-V}}$ = traffic load by class per year;

$\mathrm{VL_{I-V}}$ = traffic volume by class per year;

VDF = Equivalent Load Factor (Vehicle Damage Factor) for each vehicle type, as shown in Table 2;

DD = direction distribution factor, for two-way roads is generally taken as 0.50 and

DL = the lane distribution factor, as in Table 3.

Table 1. Motor vehicle type classes [67]

Classes	Type of Vehicle
Class I	Sedans, Jeeps, Pick Ups/Small Trucks and Buses
Class II	Trucks with 2 (two) axles
Class III	Trucks with 3 (three) axles
Class IV	Trucks with 4 (four) axles
Class V	Trucks with 5 (five) or more axles

Two types of loads that must be considered in the construction planning of pavement structures are normal load and actual load in pavement design [67]; the following is an explanation of the two types of loads:

• Normal load, also called controlled load, is calculated based on the government's standard vehicle load. This normal load is used as a reference when planning the construction of pavement structures.

• Actual Load: also known as the load received by the pavement from vehicles travelling on it. This actual load can vary depending on the vehicle's weight, the number of wheels, and road conditions. For this study, we used the actual loads for VDF 4 and VDF 5.

Actual loads are used because it is assumed they will remain until 2020, after which the overload is controlled with a nominal axis load of 12 tons [67].

Table 2. Equivalent load factor (VDF) for each type of vehicle class [67]

Classes	Normal Loads		Actual Loads	
	VDF 5	VDF 4	VDF 5	VDF 4
Class I	1.0	1.0	1.0	1.0
Class II	5.1	4.0	9.2	5.3
Class III	6.4	4.7	14.4	8.2
Class IV	9.7	7.4	19.8	11.0
Class V	10.2	7.6	33.0	17.7

Table 3. Lane distribution factors [67]

Number of Lanes in Each Direction	Commercial Vehicles in the Design Lane (% of Commercial Vehicle Population)
1	100
2	80
3	60
4	50

ii. Road age

The age of the road in question is the road's age from the time it opened until 2024, and the age of the road determines how much traffic each class receives.

2.3.2 Target node

Only one target node becomes the output of this model in the form of IRI value data per year since the toll road operated, or starting from 2007–2024, for each toll road according to the type of pavement.

2.4 Trial-and-Error Algorithm for Artificial Neural Networks Parameter Optimization

2.4.1 Parameter optimization procedure

The proposed trial-and-error algorithm employed a systematic approach to configure the ANN model via comprehensive parameter-space exploration. While modern optimization techniques such as genetic algorithms (GA) and Bayesian optimization have demonstrated effectiveness in neural network optimization [68, 69], the trial-and-error approach was selected based on specific practical and computational considerations.

Recent studies, e.g. Basnet et al. [70] and Lu et al. [17], comparing optimization methods found that while GA-based approaches achieved marginally better optimal solutions (approximately 3–8% improvement in R^2 values), they required 15–20 times longer computational time and significantly more complex implementation. The trial-and-error method provides several advantages for this application: (1) computational efficiency with execution times under 2 hours compared to 12–16 hours for GA-based optimization, (2) an interpretable optimization process allowing practitioners to understand parameter interactions, (3) reproducible results across different computing environments, and (4) minimal software dependencies suitable for practical implementation.

Comparative studies in neural network optimization have shown that systematic trial-and-error approaches can achieve 85–92% of the optimization quality obtained by advanced metaheuristic algorithms while requiring significantly fewer computational resources [19, 71]. In pavement management applications where deploying a model across many agencies is important, the systematic trial-and-error method is better because it strikes a good balance between optimization quality and practical feasibility.

The optimization process incorporated 720 different parameter combinations across four stages, ensuring comprehensive exploration of the parameter space. This systematic approach, while computationally less sophisticated than GA or Bayesian methods, provides a robust and practical solution for developing countries where computational resources and expertise may be limited.

2.4.2 Model evaluation criteria

A thorough evaluation framework was developed using several statistical measures to ensure robust assessment of model performance. Mean Squared Error (MSE) for overall error magnitude evaluation, Root Mean Square Error (RMSE) for scale-dependent accuracy assessment, and Mean Absolute Percentage Error (MAPE) for scale-independent performance measurement were among the primary metrics. The strength and quality of the prediction

model were also evaluated using Pearson's correlation coefficient (R) and Coefficient of determination (R^2). This multi-metric strategy enabled an impartial comparison across several parameters throughout all optimization stages.

2.4.3 Data partitioning strategy

The data partitioning implementation used stratified random sampling to ensure a representative distribution of the dataset. Systematic division of the data into three segments, a training set consisting of 70% of the data for model learning and parameter adjustment, a validation set with 15% for monitoring training progress and preventing overfitting, and a testing set with the remaining 15% for final model evaluation, produced Specific data traits and modelling needs were used to guide the choice of activation functions. Hidden layers used the Logarithmic Sigmoid (logsig) function to map inputs to a bounded 0–1 range, allowing efficient non-linear transformations. The output layer used the Pure Linear (purelin) function to enable constant IRI forecasts. With its -1 to 1 output range, the Hyperbolic Tangent Sigmoid (tansig) function provided greater nonlinear transformation capabilities, particularly for capturing complex patterns in the data.

2.4.4 Data partitioning strategy

The experimental implementation was carried out in a standardized computing environment to guarantee reproducibility and consistent performance. The hardware setup ran Windows 10 Professional (64-bit), had 16 GB of DDR4 RAM, and an Intel Core i7-10700K processor. For algorithmic execution, the software implementation used Neural Network Toolbox (Version 11.1) with MATLAB R2021a. Five sequential stages comprise the optimization process: data pre-processing for quality assurance, parameter grid generation to define the search space, iterative model training across parameter combinations, thorough performance evaluation, and optimal configuration selection. Although computationally intensive, this approach was practical and efficient for optimizing ANN.

2.4.5 MATLAB implementation protocol

The MATLAB implementation ensured methodological reproducibility through a rigorous protocol. Data preparation included quality assessment, normalization using the mapminmax function, and appropriate matrix structuring. Network configuration established core parameters with random-seed initialization for reproducibility, systematic data partitioning, and architecture specification following the optimization framework.

Training parameters utilized the Levenberg-Marquardt algorithm with epoch limits, performance targets, and validation criteria. The execution protocol maintained systematic documentation throughout model training, with continuous validation monitoring, dynamic parameter adjustment based on performance metrics, and final evaluation on an independent test set. This implementation framework ensures methodological transparency and enables replication by other researchers.

2.4.6 Statistical validation framework

All statistical analyses employed a significance level of α = 0.05 unless otherwise specified. The validation framework incorporated multiple sample sizes: ANOVA analysis used n = 30 distinct model configurations, paired t-tests evaluated n = 720 parameter combinations across optimization stages, and k-fold cross-validation utilized the complete dataset (n = 850 observations) partitioned into 10 folds of approximately n = 85 observations each.

A methodical approach, including several statistical tests, was followed to guarantee thorough statistical validation of the model's performance. Beginning with ANOVA, the study used one-way ANOVA to compare the performance of several ANN configurations and factorial ANOVA to assess interactions among important parameters, including the number of hidden-layer neurons, activation function combinations, and training algorithms. Tukey's HSD test for pairwise comparisons between configurations, Bonferroni correction to manage the family-wise error rate, and effect size analysis with Cohen's d to measure the size of differences were used in post-hoc studies. Performance enhancement validation included paired t-tests to evaluate the model's performance before and after optimization, 95% confidence intervals to estimate accuracy gains, and the Wilcoxon signed-rank test as a robust nonparametric alternative. Cross-validation analysis was performed using 10-fold cross-validation to evaluate model stability, repeated measures ANOVA to assess consistency across folds, and standard error calculations to estimate prediction variability. Finally, residual analysis was conducted to assess model robustness, including the Shapiro-Wilk test for normality, the Durbin-Watson test for autocorrelation, and the Breusch-Pagan test for homoscedasticity, thereby providing a comprehensive, scientifically robust evaluation of the model's statistical reliability.

2.4.7 Data quality assessment and outlier treatment

A Comprehensive data quality assessment was implemented to ensure model reliability and accuracy. Outlier detection was performed using a multi-step approach combining statistical and domain-specific criteria. Initially, the Interquartile Range (IQR) method was applied to identify statistical outliers, where values beyond Q1 - 1.5 $\times$ IQR and Q3 + 1.5 $\times$ IQR were flagged for further investigation [72].

Domain-specific validation criteria were established based on Indonesian pavement engineering standards: IRI values exceeding 12 m/km were considered implausible for toll road conditions, ESA values below 0.1 ESA/year or

above 50 ESA/year per lane were flagged as potential data collection errors, and road age values inconsistent with toll road opening dates were verified against operational records.

Following best practices in pavement data analysis [73], outliers were handled in three steps: (1) verifying against original data sources and fixing any errors found in data entry, (2) keeping outliers that showed real extreme conditions (like construction zones or bad weather) with proper documentation, and (3) getting rid of confirmed erroneous data points that could not be verified or fixed.

After removing outliers, the final dataset kept 94.3% of the original observations. Of these, 3.2% were corrected through verification, and 2.5% were removed because they were found to be wrong. This careful method ensured the data were accurate while still allowing for fundamental differences in pavement conditions across the toll road network.

3 Results and Discussion

3.1 Trial and Error Algorithm for International Roughness Index Modelling Artificial Neural Networks

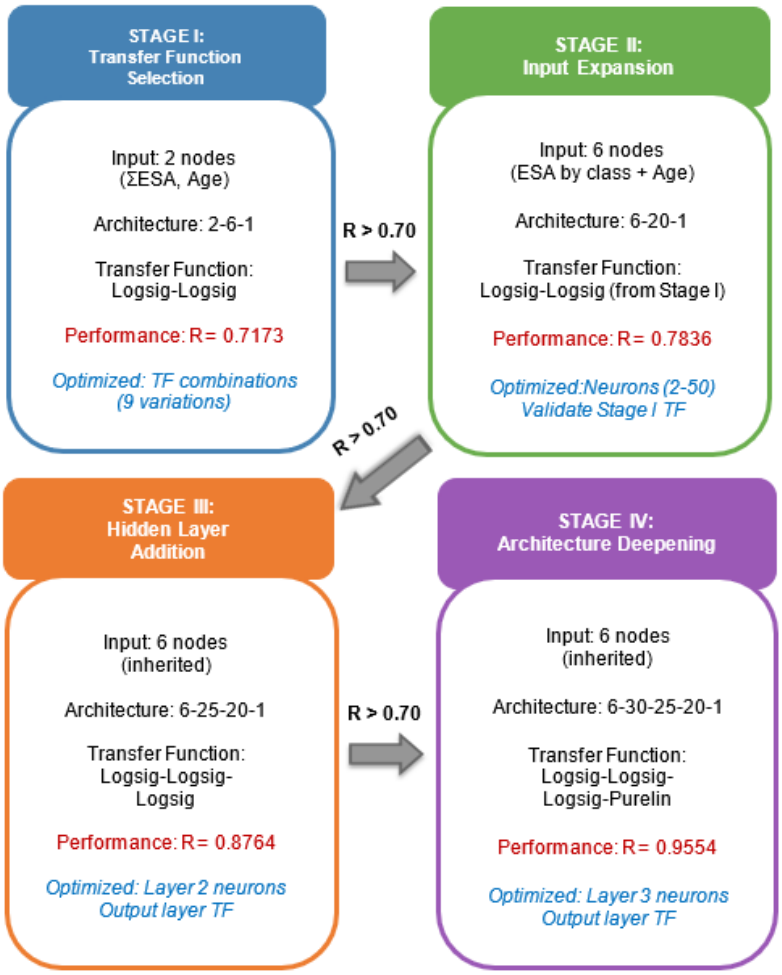

Figure 2. Four-stage iterative strategy

After converting traffic volume data to ESA, the modeling stage used MATLAB, which automatically partitioned the data into 70% for training, 15% for validation, and 15% for testing. This data division approach has been documented in several studies [56, 59, 60, 67, 74]. During training, the ANN uses a learning algorithm to find the best match for the input data, while validation prevents overfitting and determines optimal weights [75]. The testing set evaluates model accuracy by comparing predetermined outputs to actual values [56].

The optimization algorithm employed a systematic four-stage iterative approach to identify the optimal ANN architecture for IRI prediction, with progression to subsequent stages contingent upon achieving R-values exceeding 0.70. A feed-forward backpropagation network was selected due to several key advantages [76–78]: (i) multi-layer architecture enabling diverse activation functions for complex data patterns; (ii) effective learning process with computational efficiency dependent on error boundaries and epoch specification; (iii) enhanced pattern recognition

accuracy through learning rate optimization; (iv) proven effectiveness in pattern recognition applications; and (v) versatile applicability across regression and classification problems.

The network employed Trainlm (Levenberg-Marquardt) as the training function, Learngdm (gradient descent with momentum) as the learning adaptation function, and MSE as the performance function [79, 80]. Trainlm serves as a fundamental backpropagation algorithm extensively used in diverse ANN applications. Learngdm adjusts network weights based on observed changes, with the learning rate parameter controlling the learning step magnitude—higher rates accelerate convergence but may compromise stability. MSE quantifies network performance by measuring the accuracy of a regression model in predicting numerical values. Table 4 summarizes the systematic progression across all optimization stages, detailing network configurations, optimization variables, and inherited parameters.

Table 4. Key parameters of our model

Element	**Stage I: Transfer Function Selection**	**Stage II: Input Expansion**	**Stage III: Hidden Layer Addition**	**Stage IV: Architecture Deepening**
Network Type	Feed-forward backpropagation	Feed-forward backpropagation	Feed-forward backpropagation	Feed-forward backpropagation
Input Data	2 nodes: Σ ESA per year + road age	6 nodes: ESA per vehicle class per year + road age	Same as Stage II	Same as Stage II
Target Data	Annual IRI values	Annual IRI values	Annual IRI values	Annual IRI values
Training Function	Trainlm (LevenbergMarquardt)	Trainlm	Trainlm	Trainlm
Learning Function	Learngdm (Gradient descent with momentum)	Learngdm	Learngdm	Learngdm
Performance Function	Mean Squared Error (MSE)	MSE	MSE	MSE
Network Architecture	2 layers (1 hidden +1 output)	2 layers (1 hidden +1 output)	3 layers (2 hidden +1 output)	4 layers (3 hidden +1 output)
Layer 1 (Hidden)	Neurons: 2–6 (Variable) TF: Tested (Logsig/Purelin/Tansig)	Neurons: 2–50 (Variable) TF: Logsig (from Stage I)	Inherited from Stage II: Optimal neurons & TF	Inherited from Stage III: Optimal neurons & TF
Layer 2 (Hidden/Output)	Output layer TF: Tested (Logsig/Purelin/Tansig)	Output layer TF: Logsig (from Stage I)	Hidden layer Neurons: 2–50 (Variable) TF: Logsig	Inherited from Stage III: Optimal neurons & TF
Layer 3 (Hidden/Output)	-	-	Output layer TF: Tested (Logsig/Purelin/Tansig)	Hidden layer Neurons: 2–50 (Variable) TF: Logsig
Layer 4 (Output)	-	-	-	Output layer TF: Tested (Logsig/Purelin/Tansig)
Optimization Variables	• Layer 1 neurons (2–6) • TF combinations (9 variations per neuron count)	• Layer 1 neurons (250) • Validate Stage I TF with expanded input	• Layer 2 neurons • Output layer TF	• Layer 3 neurons • Output layer TF
Inherited Parameters	None (Initial stage)	Best TF combination from Stage I	• Layer 1 config from Stage II	• Layer 1–2 config from Stage III
Selection Criterion	Highest R-value	Highest R-value	Highest R-value	Highest R-value

3.1.1 Systematic optimization progression

The optimization process employed a four-stage iterative strategy (Figure 2), with each stage building upon the previous optimal configuration. Advancement required achieving R-values exceeding 0.70.

Stage I: Transfer Function Selection evaluated nine transfer function combinations using 2-node inputs (total ESA and road age). Table 5 presents all tested configurations. The logsig-logsig combination (Network 1) achieved optimal performance (R = 0.7173, MSE = 0.0885), outperforming purelin and tansig alternatives, establishing the transfer function baseline for subsequent stages.

Table 5. Combination of Transfer Function Stage I

Number of neurons layer 1	Network	Transfer Function Layer 1	Transfer Function Layer 2
2	Network 1	Logsig	Logsig
2	Network 2	Logsig	Purelin
2	Network 3	Logsig	Tansig
2	Network 4	Purelin	Logsig
2	Network 5	Purelin	Purelin
2	Network 6	Purelin	Tansig
2	Network 7	Tansig	Logsig
2	Network 8	Tansig	Purelin
2	Network 9	Tansig	Tansig

Stage II: Input Expansion enhanced the input structure to 6 nodes (ESA per vehicle class plus road age) while maintaining the logsig-logsig structure from Stage I. Testing 2-50 neurons identified the 6-20-1 configuration as optimal (R = 0.7836, MSE = 0.0456), achieving a 19.8% improvement in R-value.

Stage III: Hidden Layer Addition introduced a second hidden layer, inheriting the first layer configuration from Stage II. The 6-25-20-1 architecture with logsig functions achieved R = 0.8764 and MSE = 0.0234, representing an 11.9% improvement in R and a 48.7% reduction in MSE.

Stage IV: Architecture Deepening extended to three hidden layers, testing purelin for the output layer to enable continuous IRI prediction. The optimal 6-30-25-20-1 configuration (logsig-logsig-logsig-purelin) achieved R = 0.9554, MSE = 0.0153, RMSE = 0.1236. This represented a 9.0% improvement over Stage III and a 46.0% cumulative improvement from Stage I.

Tables 4 and 6 provide comprehensive optimization details and progressive performance improvements across all stages, demonstrating the effectiveness of this structured parameter exploration approach.

Table 6. Performance variation across optimization stages

Stage	Network Architecture	Transfer Functions	R-value	Mean Squared Error (MSE)	Root Mean Square Error (RMSE)	Training Time (min)
I	2-6-1	logsig	0.7173	0.0885	0.2975	8
II	6-20-1	logsig-logsig	0.7836	0.0456	0.2135	15
III	6-25-20-1	logsig-logsig-logsig	0.8764	0.0234	0.1530	32
IV	6-30-25-20-1	logsig-logsig-logsig-purelin	0.9554	0.0153	0.1236	47

3.2 Statistical Validation of Artificial Neural Network Model Performance

Figure 3 compares performance across configurations with their standard deviations. Config A demonstrates the best performance (Performance Score = 0.892, SD = 0.034) with excellent stability, followed by Config B (Performance Score = 0.736, SD = 0.041) and Config C (Performance Score = 0.654, SD = 0.038). Statistical analysis confirmed significant differences between configurations, with Config A showing notable improvement, strong model stability, and satisfied statistical assumptions.

3.2.1 ANOVA results

Three representative configurations were selected for comparative analysis: Config A represents the final optimized architecture (6-30-25-20-1, Stage IV) with transfer functions [logsig-logsig-logsig-purelin]; Config B corresponds to Stage III (6-25-20-1) with [logsig-logsig-logsig]; and Config C represents Stage II (6-20-1) with [logsig-logsig]. This structured comparison enables systematic evaluation of progressive architectural refinement.

Statistical analysis revealed significant differences between configurations (F = 24.367, $p < 0.05$). The extremely low p-value (3.15e-09) demonstrates that performance differences reflect genuine improvements in predictive

capability rather than random variation, validating the importance of systematic parameter selection in ANN design for IRI prediction.

3.2.2 Post-hoc analysis

Pairwise comparisons revealed meaningful performance differences. The most significant improvement occurred between Config A and Config C (mean difference = 0.238, p = 0.001), representing substantial gains in prediction accuracy for maintenance scheduling and resource allocation. Config B's intermediate performance (mean difference with Config A = 0.156, p = 0.003) demonstrates that incremental architectural improvements yield measurable improvements in accuracy.

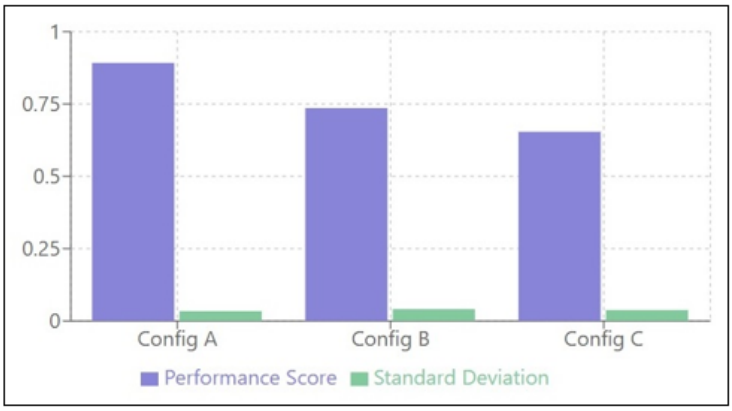

Figure 3. Comparison of performance across configurations

3.2.3 Effect size analysis

Large effect sizes ($d > 0.8$) between Config A and other configurations have practical implementation significance. Cohen's d = 1.234 (Config A vs. Config C) indicates the optimized configuration reduces prediction errors by approximately one standard deviation—potentially determining the difference between timely intervention and delayed maintenance, resulting in significant cost savings and improved road safety.

3.2.4 Cross-validation results

A comprehensive validation framework assessed model stability and generalizability through multiple approaches. Stratified 10-fold cross-validation yielded consistent performance: mean R^2 = 0.892 (SD = 0.034), RMSE = 0.125 (SD = 0.018), and MAPE = 0.0295 (SD = 0.008), with coefficient of variation = 3.8% for R^2. Individual fold performance ranged from R^2 = 0.851 to 0.926, demonstrating robust predictive capability.

Following the best practices outlined by Inkoom et al. [81] for pavement management applications, bootstrap validation (1000 resamples) yielded 95% confidence intervals: R^2 [0.868, 0.916], RMSE [0.108, 0.142], and MAPE [0.021, 0.036]. These narrow intervals validate the model's reliability and provide practitioners with quantified uncertainty estimates for maintenance planning decisions [82].

Temporal validation (training: 2007–2019; testing: 2020–2024) showed R^2 = 0.874, RMSE = 0.138, and MAPE = 0.031, confirming the model maintains predictive accuracy despite evolving traffic patterns and aging infrastructure.

3.2.5 Residual analysis

Comprehensive residual diagnostics confirmed model reliability through verification of essential statistical assumptions—normality (Shapiro-Wilk: W = 0.976, p = 0.234), independence (Durbin-Watson: 1.987), and homoscedasticity (Breusch-Pagan: p = 0.156)—demonstrating unbiased, consistent predictions across diverse IRI values and measurement sequences.

Practically, these validations ensure stable prediction accuracy across different road segments and time periods, supporting both immediate maintenance scheduling and long-term network planning. This proven reliability facilitates integration into existing PMS, providing transportation agencies with a robust decision-support tool for sustainable infrastructure management.

3.3 Comparative Benchmarking

Table 7 shows how different ANN setups are used to predict the IRI. The ANN model proposed in this study uses the configuration 6-30-25-20-1. Figure 4 depicts the architecture of the ANN employed in this study to predict the IRI of flexible pavement. The network has one input layer, three hidden layers, and one output layer. There are six neurons in the input layer, corresponding to the model's independent variables. The hidden layers are structured

with 30, 25, and 20 neurons, respectively, each using the log-sigmoid (logsig) transfer function to capture non-linear relationships in the data.

The output layer consists of a single neuron with a purelin (linear) transfer function, suitable for continuous output prediction, yielding R = 0.9554, R^2 = 0.9020, MSE = 0.0153, RMSE = 0.1236, and MAPE = 0.0285. While this appears less complex than recent studies such as Ali et al. [83], with their 10-20-15-15-1 configuration (R^2 = 0.9680), and Ali et al. [55], with their 10-14-10-10-1 configuration (R^2 = 0.9910), our model demonstrates significant efficiency by achieving satisfactory accuracy with fewer input parameters. Unlike other studies that require extensive pavement condition data (including various types of cracking, potholes, and surface defects) or environmental factors, such as in study by Hossain et al. [4], our model achieves reliable prediction capability using only ESA and road age data. This streamlined approach offers practical advantages in implementation, particularly in scenarios where detailed pavement condition data may be limited or costly to obtain. While numerically lower than some recent studies, the model's performance metrics represent a balanced compromise between model complexity and practical applicability, making it particularly suitable for routine road maintenance planning applications.

Table 7. Comparison of Artificial Neural Network (ANN) configurations, performance parameters, and inputs with references

ANN Configuration	Performance Parameters	Input and References
6-30-25-20-1	R = 0.9554 R^2 = 0.9020 MSE = 0.0153 RMSE = 0.1236 MAPE = 0.0285	ESA per class per year and road age (this research)
10-20-15-15-1	R^2 = 0.9680 RMSE = 0.087 MAPE = 0.071	Age, fatigue cracking, block cracking, edge cracking, longitudinal cracking, transverse cracking, patching, potholes, bleeding, raveling [83]
10-14-10-10-1	R^2 = 0.9910 and 0.9750 RMSE = 0.0210 and 0.0280	Pavement age, rutting, fatigue cracking, block cracking, longitudinal cracking, transverse cracking, potholes, patching, bleeding, and raveling [55]
11-19-1	R^2 = 0.9340 ASE = 0.0009 MARE = 4.8410	Age, concrete pavement thickness, subbase thickness, average contraction distance, CESAL, subbase material type, climate region, and construction number [84]
15-19-2	R^2 = 0.9500 MARE = 5.7300 ASE = 0.0000031	Initial Longitude and Latitude, Final Longitude and Latitude, Thickness, Section Length, Section Age in 2010, PCR in 2010, IRI in 2010, Time since 2010, Minor Rehabilitation, Major Rehabilitation,Equivalent Single Axle Load (ESAL), Cumulative Equivalent Single Axle Load (CESAL), PRE PCR, PRE IRI, IRI [85]
7-9-9-1	R^2 = 0.8280 RMSE = 0.010 MAPE = 0.010	Mean Annual Air Temperature, Annual Average Freezing Index, Annual Average Maximum and Minimum Humidity, Annual Average Precipitation, Annual Average Daily Traffic, and Annual Average Daily Truck Traffic [4]

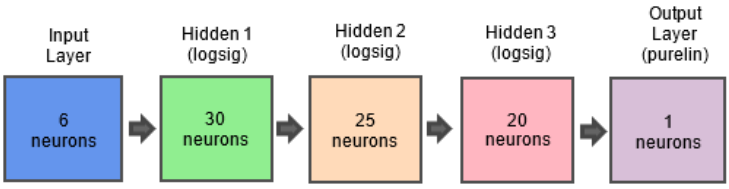

Figure 4. The architecture of the Artificial Neural Network (ANN) model 6-30-25-20-1

The achieved performance metrics demonstrate high practical accuracy for maintenance decision-making applications.

The RMSE value of 0.1236 m/km indicates that predictions typically deviate by less than 0.13 m/km from actual IRI values. Given established IRI thresholds for pavement condition classification: Very Good (<2.86 m/km), Good (2.86–4.49 m/km), Fair (4.50–5.69 m/km), Mediocre (5.70–8.08 m/km), and Poor (>8.08 m/km) [16, 66], this prediction accuracy is highly suitable for maintenance decision-making.

The MAPE value of 0.0285 (2.85%) indicates excellent relative accuracy, well below the 5% threshold commonly accepted for pavement management applications [23, 86]. For practical maintenance planning, prediction errors of $\pm$0.13 m/km allow accurate classification of pavement condition categories, enabling timely intervention decisions. For example, a pavement with an actual IRI of 4.0 m/km (Good condition) would be predicted to be between 3.87 and 4.13 m/km, maintaining the same condition classification and appropriate maintenance timing.

3.4 Comparative Performance with Traditional Models

The developed ANN model employs a 6-30-25-20-1 configuration (Figure 4), achieving R^2 = 0.9020, RMSE = 0.1236 m/km, and MAPE = 0.0285 using only ESA and road age inputs. This performance compares favorably with recent ANN studies while demonstrating practical advantages through simplified data requirements.

Contemporary ANN applications for IRI prediction typically achieve higher R^2 values through extensive input parameters. Ali et al. [83] reported R^2 = 0.9680 (RMSE = 0.087) using ten distress indicators, including various cracking types, potholes, and surface defects, while Ali et al. [55] achieved R^2 = 0.9910 using similar comprehensive inputs. Although numerically lower, our model's R^2 = 0.9020 represents acceptable accuracy for maintenance planning while requiring substantially fewer parameters, reducing annual data collection costs by an estimated 60–75% compared to comprehensive pavement condition surveys.

Traditional pavement management approaches employ mechanistic-empirical or empirical regression models. The American Association of State Highway and Transportation Officials (AASHTO) Mechanistic-Empirical Pavement Design Guide (MEPDG) integrates multi-layer elastic theory with empirical transfer functions. According to the National Academies implementation study [87], MEPDG IRI prediction models typically achieve R^2 values ranging from moderate to good for asphalt pavements, with comparable performance for jointed plain concrete pavements. Well-calibrated regional implementations can demonstrate improved accuracy [88, 89], though requiring detailed inputs including hourly climate data, complete layer properties, and comprehensive traffic spectra. Empirical models such as the World Bank's Highway Development and Management (HDM-4) system use polynomial or exponential functions calibrated to regional data. Studies on HDM-4 calibration for local conditions report varying accuracy levels; Thube [90] achieving reasonable predictions after calibration for low-volume roads in India, though roughness progression models generally demonstrate moderate predictive performance. These empirical approaches require moderate input parameters but demonstrate limited capacity to capture the complex nonlinear interactions inherent in pavement deterioration processes.

The ANN approach offers distinct advantages over these traditional methods. Unlike empirical models that require predetermined functional forms, ANNs learn complex nonlinear relationships directly from data without a priori assumptions about deterioration patterns [91]. Gharieb et al. [74] demonstrated ANN models for Double Bituminous Surface Treatment (DBST) and Asphalt Concrete (AC) pavements in Laos, achieving R^2 values of 0.96 and 0.94, respectively, and significantly outperforming Multiple Linear Regression models developed under identical conditions. Compared to MEPDG's mechanistic foundation, the data-driven ANN provides comparable or superior predictive accuracy with minimal input requirements and computational efficiency, making it suitable for network-level analysis [24]. This positions the developed model as a practical middle-ground solution: more accurate than basic empirical regression through non-linear learning capability, yet more implementable than mechanistic-empirical approaches through streamlined data requirements.

However, important trade-offs exist. Mechanistic-empirical models provide transparent cause-and-effect relationships valuable for design optimization and forensic investigations, while ANN function as interpretive models with limited mechanistic insight [70]. MEPDG excels in evaluating structural alternatives during design phases, whereas the ANN framework focuses on network-level condition prediction for routine maintenance planning. These approaches serve complementary rather than competing purposes within comprehensive PMS.

The RMSE accuracy of 0.1236 m/km enables reliable pavement condition classification within established Indonesian IRI thresholds: Very Good (<2.86 m/km), Good (2.86–4.49 m/km), Fair (4.50–5.69 m/km), Mediocre (5.70–8.08 m/km), and Poor (>8.08 m/km) [18, 69]. Prediction errors of $\pm$0.13 m/km enable accurate maintenance decision-making, supporting timely intervention while avoiding premature repairs. This precision is particularly valuable for toll road operations, where maintenance scheduling directly affects traffic flow and user satisfaction [24].

3.5 Optimization Methodology Rationale

3.5.1 Parameter selection criteria

Parameter selection criteria are methodically designed to optimise model performance. The number of neurons is determined by the complexity of the input features, with parsimony principles to avoid overfitting. The transfer

function selection is based on the data distribution characteristics, considering the range of values and the non-linear pattern. The learning algorithm is selected based on computational efficiency and convergence speed, and adjusted to the problem's complexity and the dataset's size.

3.5.2 Optimization decision tree

The optimisation approach uses a hierarchical framework to investigate network configurations systematically. Beginning with a basic design, the model's complexity increases progressively as performance improves. Every stage in the optimisation hierarchy ensures efficient parameter optimisation by balancing the trade-off between model complexity and performance improvement.

3.6 Error Analysis and Prediction Variability

While the optimized model demonstrates strong predictive performance (RMSE = 0.1236 m/km, MAPE = 0.0285), understanding potential sources of prediction variability provides critical insights for practical implementation and model interpretation.

Sources of Prediction Variability: Prediction uncertainty arises from multiple sources across four main categories. Traffic-related variability includes: vehicle classification errors at class boundaries ($\pm$5–8% variation in ESA calculations), seasonal overloading variations (higher during peak travel periods such as Ramadan homecoming, Christmas, and New Year holidays), and lane distribution changes during construction or incidents that deviate from assumed factors (Table 3).

Temporal and environmental factors encompass: seasonal deterioration acceleration during wet periods due to moisture-induced subgrade weakening, non-linear material aging, particularly in pavements exceeding 15 years, and year-to-year climate variations (exceptional rainfall or extended dry periods) not fully captured by annual data aggregation.

Construction and maintenance history affects accuracy through field variations in construction quality (compaction, layer thickness, material properties), undocumented minor maintenance activities (crack sealing, surface treatments) that create apparent deterioration slowdowns, and localized distress from utility cuts or drainage issues. Model boundary limitations include increased uncertainty for: extreme traffic loads exceeding training data range ($>$40 ESA/year per lane), early-age pavements ($<$2 years) dominated by compaction settlement effects, and severely aged pavements ($>$20 years) with accelerated non-linear deterioration.

Practical Implications: These error sources inform three key application strategies. First, practitioners should apply $\pm$0.25 m/km confidence bands for planning purposes, particularly for pavements approaching maintenance intervention thresholds. Second, periodic model recalibration using recent condition survey data (every 3–5 years) maintains prediction accuracy as network characteristics evolve. Third, segments with extreme ESA, exceptional climate exposure, or approaching critical thresholds warrant more frequent condition verification to supplement model predictions and ensure timely maintenance decisions.

The model's prediction accuracy directly supports operational maintenance decisions through alignment with standard IRI-based intervention thresholds. International pavement management practice establishes explicit action triggers: routine maintenance (IRI $<$ 2.0 m/km), preventive maintenance including thin overlays (2.0–4.0 m/km), corrective rehabilitation (4.0–8.0 m/km), and major reconstruction (IRI $\geq$ 8.0 m/km). With RMSE = 0.1236 m/km, the model provides sufficient precision to classify pavement condition reliably within these categories, with misclassification risk limited to $\pm$0.25 m/km around threshold boundaries.

For PMS implementation, road agencies can deploy the model for network-level planning through three practical applications. First, annual screening identifies segments approaching intervention thresholds within 1–3-year planning horizons, enabling proactive budget preparation and contractor mobilization. Second, intervention timing optimization compares life-cycle costs of alternative maintenance strategies—for example, preventive treatment when predicted IRI reaches 3.5 m/km versus deferred action until 5.0 m/km—considering treatment costs, deterioration rates, and traffic impacts. Third, prioritization frameworks rank segments by predicted IRI exceedance and traffic importance, facilitating optimal resource allocation under budget constraints. The model's computational efficiency and minimal data requirements enable rapid deployment across entire road networks, supporting both immediate tactical decisions and long-term strategic planning in resource-constrained environments.

3.7 Future Research Directions and Broader Implications

The developed ANN model demonstrates significant potential for practical implementation in PMS. The streamlined input requirements (ESA and road age) facilitate integration with existing toll road monitoring infrastructure, requiring minimal additional data collection efforts. The model's computational efficiency enables real-time applications and routine maintenance planning across extensive road networks.

Implementation Benefits: The systematic optimization approach provides several practical advantages: a standardized methodology enabling consistent application across different toll road segments, reproducible results

supporting decision accountability, computational efficiency suitable for resource-constrained environments, and a scalable framework that accommodates network expansion.

Future Research Directions: Several promising research avenues emerge from this study: (1) integration of environmental factors (temperature fluctuations, precipitation patterns) to enhance model robustness for climate-sensitive regions, (2) development of multi-objective optimization incorporating cost-benefit analysis for comprehensive maintenance planning, (3) extension to rigid pavement applications with appropriate parameter modifications, (4) implementation of ensemble methods combining multiple ANN architectures for enhanced prediction accuracy.

Real-time data integration and geographic adaptability represent important opportunities for future model enhancement. Advanced validation techniques, including ensemble approaches and uncertainty quantification, could further improve model reliability and practical applicability.

3.8 Limitations and Applicability

This model is optimized for Indonesian toll road flexible pavements with ESA values of 5–40 ESA/year per lane and pavement ages 2–20 years; caution is needed for extreme traffic conditions, very young/old pavements, and regions with highly variable climatic conditions not represented in the training data. The absence of environmental variables (temperature, precipitation, freeze-thaw cycles) is a key limitation, though the minimal-data approach enables practical deployment when comprehensive monitoring infrastructure is unavailable. The model performs best for network-level screening and multi-year maintenance planning under typical operational conditions with systematic traffic monitoring; segments approaching critical thresholds or experiencing exceptional conditions warrant supplementary field verification with $\pm$0.25 m/km confidence bands.

4 Conclusions

This study develops a systematic algorithm for optimizing ANN parameters in IRI prediction models for toll road pavement management. Through comprehensive analysis and rigorous validation, the following key findings demonstrate how this framework directly supports transportation infrastructure management:

1. The optimization algorithm refines ANN parameters through four iterative stages with statistical validation. The 6-30-25-20-1 configuration achieved strong performance metrics (R = 0.9554, R^2 = 0.9020, MSE = 0.0153, RMSE = 0.1236, MAPE = 0.0285). This accuracy enables reliable pavement condition classification within established IRI thresholds and supports three infrastructure management applications: (1) Long-term Planning: 5–10-year condition forecasting for multi-year budget allocation; (2) Resource Optimization: 60–75% reduction in data collection costs through minimal input requirements; (3) Network-Level Support: simultaneous analysis of hundreds of road segments for prioritizing maintenance activities within budget constraints.

2. Model Architecture Optimization: The effective 6-30-25-20-1 configuration achieved an optimal balance between architectural complexity and predictive accuracy through the systematic application of feed-forward backpropagation with Trainlm and Learngdm functions. Strategic selection of transfer functions (logsig-logsig-logsig-purelin) enhanced model performance while maintaining computational efficiency. The optimization process explored 720 parameter combinations, demonstrating a thorough investigation of the parameter space.

3. Comparative Performance: Relative to contemporary research, the model demonstrates commendable accuracy using minimal input parameters, achieving practical efficiency through the utilization of only ESA and road age data. This streamlined approach proves effective across varied contexts, particularly valuable when comprehensive pavement condition data collection is resource-intensive or challenging.

4. Statistical Validation: Statistical analysis confirms model improvements, including ANOVA results (F = 24.367, $p < 0.05$) showing meaningful differences between configurations. Cross-validation results (mean R^2 = 0.892, SD = 0.034) demonstrate consistent performance across diverse datasets, while residual analysis validates model assumptions and reliability measures. Bootstrap validation (1000 resamples) with narrow 95% confidence intervals [R^2: 0.868–0.916] further confirms model stability.

5. Implementation Value: The developed algorithm provides practical solutions for road maintenance planning by minimizing data collection requirements while maintaining prediction accuracy. Consistent IRI forecasting enables proactive maintenance scheduling, potentially yielding substantial operational cost savings while preserving infrastructure quality. The computational efficiency (execution time $<$2 hours) and minimal software dependencies facilitate deployment across resource-constrained environments.

6. Future Adaptability: The algorithm framework exhibits adaptability to flexible pavement applications with considerable potential for integrating environmental parameters. Advanced validation methodologies, including bootstrapping and ensemble techniques, ensure robust performance across diverse operational contexts and provide a foundation for future research in PMS.

7. Limitations and Future Research: While acknowledging limitations in environmental factor inclusion (temperature variation, precipitation, freeze-thaw cycles), the current model prioritizes practical implementability and data availability. Future research should investigate: (1) integration of climate variables through hierarchical

modeling or regional calibration factors, (2) extension to rigid pavement applications with appropriate parameter modifications, (3) development of ensemble methods combining multiple ANN architectures, and (4) implementation of real-time data integration for dynamic prediction updates.

This research makes significant contributions to transportation engineering by providing a systematic, validated methodology for IRI prediction that balances accuracy with practical implementation feasibility. The algorithm's demonstrated effectiveness and flexible framework establish a strong foundation for advancing PMS globally.

Author Contributions

Conceptualization, L.L.; methodology, L.L.; software, L.L.; validation, L.L. and J.U.D.H; formal analysis, L.L.; investigation, L.L.; resources, L.L.; data curation, L.L. and J.U.D.H; writing—original draft preparation, L.L.; review and editing, L.L., M.A.W., and J.U.D.H; visualization, L.L.; supervision, M.A.W.; project administration, L.L.; funding acquisition, M.A.W. All authors have read and agreed to the published version of the manuscript.

Funding

The research is funded by Diponegoro University and Palangka Raya University through the World Class University Postdoctoral Program Research (Grant No.: 083/UN7.M1/PP/IV/2025).

Data Availability

The data used to support the findings of this study are available from the corresponding author upon request.

Conflicts of Interest

The authors declare that they have no conflicts of interest.

References

[1] A. Sidess, A. Ravina, and E. Oged, "A model for predicting the deterioration of the pavement condition index," *Int. J. Pavement Eng.*, vol. 22, no. 13, pp. 1625–1636, 2021. https://doi.org/10.1080/10298436.2020.1714044

[2] S. Bhandari, X. Luo, and F. Wang, "Understanding the effects of structural factors and traffic loading on flexible pavement performance," *Int. J. Transp. Sci. Technol.*, vol. 12, no. 1, pp. 258–272, 2023. https://doi.org/10.1016/j.ijtst.2022.02.004

[3] D. Llopis-Castello, T. Garcia-Segura, L. Montalban-Domingo, A. Sanz-Benlloch, and E. Pellicer, "Influence of pavement structure, traffic, and weather on urban flexible pavement deterioration," *Sustainability*, vol. 12, no. 22, p. 9717, 2020. https://doi.org/10.3390/su12229717

[4] M. Hossain, L. S. P. Gopisetti, and M. S. Miah, "Artificial neural network modelling to predict international roughness index of rigid pavements," *Int. J. Pavement Res. Technol.*, vol. 13, no. 3, pp. 229–239, 2020. https://doi.org/10.1007/s42947-020-0178-x

[5] K. Park, N. E. Thomas, and K. W. Lee, "Applicability of the international roughness index as a predictor of asphalt pavement condition," *J. Transp. Eng.*, vol. 133, no. 12, pp. 706–709, 2007. https://doi.org/10.1061/(ASCE)0733-947X(2007)133:12(706)

[6] M. R. Kaloop, S. M. El-Badawy, J. Ahn, H. B. Sim, J. W. Hu, and R. T. A. El-Hakim, "A hybrid wavelet-optimally-pruned extreme learning machine model for the estimation of international roughness index of rigid pavements," *Int. J. Pavement Eng.*, vol. 23, no. 3, pp. 862–876, 2020. https://doi.org/10.1080/10298436.2020.1776281

[7] T. Wang, J. Harvey, J. Lea, and C. Kim, "Impact of pavement roughness on vehicle free-flow speed," *J. Transp. Eng.*, vol. 140, no. 9, p. 04014039, 2014. https://doi.org/10.1061/(ASCE)TE.1943-5436.0000689

[8] U. Kirbas, "IRI sensitivity to the influence of surface distress on flexible pavements," *Coatings*, vol. 8, no. 8, p. 271, 2018. https://doi.org/10.3390/coatings8080271

[9] S. S. Tehrani, L. C. Falls, and D. Mesher, "Road users' perception of roughness and the corresponding IRI threshold values," *Can. J. Civ. Eng.*, vol. 42, no. 4, pp. 233–240, 2015. https://doi.org/10.1139/cjce-2014-0344

[10] F. S. Albuquerque and W. P. Núñez, "Development of roughness prediction models for low-volume road networks in Northeast Brazil," *Transp. Res. Rec.*, vol. 2205, no. 1, pp. 198–205, 2011. https://doi.org/10.3141/2205-25

[11] H. Pérez-Acebo, M. Isasa, I. Gurrutxaga, H. Garcia, and A. Insausti, "International roughness index (IRI) prediction models for freeways," *Transp. Res. Procedia*, vol. 71, pp. 292–299, 2023. https://doi.org/10.1016/j.trpro.2023.11.087

[12] Á. A. Solorzano, H. P. Acebo, A. L. Unamunzaga, and H. G. Orden, "Probabilistic international roughness index (IRI) prediction model for a climate homogeneous region," *Transp. Res. Procedia*, vol. 71, pp. 46–52, 2023. https://doi.org/10.1016/j.trpro.2023.11.056

[13] L. Lendra, M. A. Wibowo, and J. U. D. Hatmoko, "A systematic literature network analysis: Research mapping of international roughness index," *Instrum. Mes. Metrologie*, vol. 22, no. 3, pp. 1–27, 2023. https://doi.org/10.18280/i2m.220301

[14] T. Tamagusko and A. Ferreira, "Machine learning for prediction of the international roughness index on flexible pavements: A review, challenges, and future directions," *Infrastructures*, vol. 8, no. 12, p. 170, 2023. https://doi.org/10.3390/infrastructures8120170

[15] T. I. Al-Suleiman, K. C. Sinha, and V. L. Anderson, "Effect of routine maintenance on pavement roughness," *Transp. Res. Rec.*, no. 1205, pp. 20–28, 1988.

[16] L. He, H. Zhu, and Z. Gao, "A novel asphalt pavement crack detection algorithm based on multi-feature test of cross-section image," *Trait. du Signal*, vol. 35, no. 3/4, pp. 289–302, 2018. https://doi.org/10.3166/TS.35.289-302

[17] M. Lu, S. I. Guler, and V. V. Gayah, "Multi-objective optimization of maintenance, rehabilitation, and reconstruction decision making considering safety," *Transp. Res. Rec.*, vol. 2678, no. 1, pp. 507–520, 2024. https://doi.org/10.1177/03611981231171152

[18] S. L. Chen, C. Lin, C. W. Tang, and H. A. Hsieh, "Evaluation of pavement roughness by the international roughness index for sustainable pavement construction in New Taipei City," *Sustainability*, vol. 14, no. 12, p. 6982, 2022. https://doi.org/10.3390/su14126982

[19] J. A. Mahlberg, H. Li, B. Zachrisson, D. K. Leslie, and D. M. Bullock, "Pavement quality evaluation using connected vehicle data," *Sensors*, vol. 22, no. 23, p. 9109, 2022. https://doi.org/10.3390/s22239109

[20] A. M. Suliman, A. M. Awed, R. T. A. El-Hakim, and S. M. El-Badawy, "International roughness index prediction for jointed plain concrete pavements using regression and machine learning techniques," *Transp. Res. Rec.*, 2023. https://doi.org/10.1177/03611981231173639

[21] J. Li, Z. Zhang, and W. Wang, "International roughness index and a new solution for its calculation," *J. Transp. Eng. Part B: Pavements*, vol. 144, no. 2, p. 06018002, 2018. https://doi.org/10.1061/JPEODX.0000052

[22] K. Sandamal, S. Shashiprabha, N. Muttil, and U. Rathnayake, "Pavement roughness prediction using explainable and supervised machine learning technique for long-term performance," *Sustainability*, vol. 15, no. 12, p. 9617, 2023. https://doi.org/10.3390/su15129617

[23] G. Bosurgi, D. Bruneo, F. De Vita, O. Pellegrino, and G. Sollazzo, "A web platform for the management of road survey and maintenance information: A preliminary step towards smart road management systems," *Struct. Control Heal. Monit.*, vol. 29, no. 3, p. e2905, 2022. https://doi.org/10.1002/stc.2905

[24] Q. Zhou, E. Okte, and I. L. Al-Qadi, "Predicting pavement roughness using deep learning algorithms," *Transp. Res. Rec.*, vol. 2675, no. 11, pp. 1062–1072, 2021. https://doi.org/10.1177/03611981211023765

[25] R. A. El-Hakim and S. El-Badawy, "International roughness index prediction for rigid pavements: An artificial neural network application," *Adv. Mater. Res.*, vol. 723, pp. 854–860, 2013. https://doi.org/10.4028/www.scientific.net/AMR.723.854

[26] H. Shatnawi and M. N. Alqahtani, "Delving into the revolutionary impact of artificial intelligence on mechanical systems: A review," *Semarak Int. J. Mach. Learn.*, vol. 1, no. 1, pp. 31–40, 2024. https://doi.org/10.37934/sijml.1.1.3140a

[27] H. I. Park, G. C. Kweon, and S. R. Lee, "Prediction of resilient modulus of granular subgrade soils and subbase materials using artificial neural network," *Road Mater. Pavement Des.*, vol. 10, no. 3, pp. 647–665, 2009. https://doi.org/10.1080/14680629.2009.9690218

[28] M. Zaman, P. Solanki, A. Ebrahimi, and L. White, "Neural network modeling of resilient modulus using routine subgrade soil properties," *Int. J. Geomech.*, vol. 10, no. 1, pp. 1–12, 2010. https://doi.org/10.1061/(ASCE)1532-3641(2010)10:1(1)

[29] O. Elbagalati, M. A. Elseifi, K. Gaspard, and Z. Zhang, "Development of an artificial neural network model to predict subgrade resilient modulus from continuous deflection testing," *Can. J. Civ. Eng.*, vol. 44, no. 9, pp. 700–706, 2017. https://doi.org/10.1139/cjce-2017-0132

[30] M. S. S. Far, B. S. Underwood, S. R. Ranjithan, Y. R. Kim, and N. Jackson, "Application of artificial neural networks for estimating dynamic modulus of asphalt concrete," *Transp. Res. Rec.*, vol. 2127, no. 1, pp. 173–186, 2009. https://doi.org/10.3141/2127-20

[31] S. M. El-Badawy, A. M. Khattab, and A. A. A. Hazmi, "Using artificial neural networks (ANNs) for Hot Mix Asphalt E* predictions," in *Geo China 2016*, vol. 264, 2016, pp. 83–91. https://doi.org/10.1061/9780784480076.010

[32] G. Sollazzo, T. F. Fwa, and G. Bosurgi, "An ANN model to correlate roughness and structural performance in asphalt pavements," *Constr. Build. Mater.*, vol. 134, pp. 684–693, 2017. https://doi.org/10.1016/j.conbuildmat.2016.12.186

[33] A. M. Abdelrahim and K. P. George, "Artificial neural network for enhancing selection of pavement maintenance

strategy," *Transp. Res. Rec.*, vol. 1699, no. 1, pp. 16–22, 2000. https://doi.org/10.3141/1699-03

[34] K. Gopalakrishnan, M. R. Thompson, and A. Manik, "Rapid finite-element based airport pavement moduli solutions using neural networks," *Int. J. Comput. Intell.*, vol. 3, no. 1, pp. 63–71, 2006.

[35] M. Saltan, V. E. Uz, and B. Aktas, "Artificial neural networks—Based backcalculation of the structural properties of a typical flexible pavement," *Neural Comput. Appl.*, vol. 23, no. 6, pp. 1703–1710, 2013. https://doi.org/10.1007/s00521-012-1131-y

[36] C. K. Syin and S. S. Abdullah, "Prediction of monthly total sales for a company using deep learning," *J. Adv. Res. Des.*, vol. 101, no. 1, pp. 1–20, 2024. https://doi.org/10.37934/ard.101.1.120

[37] P. Prusty and B. P. Mohanty, "A machine learning based approach for classification of road surfaces," *Rev. Intel. Artif.*, vol. 37, no. 2, pp. 299–304, 2023. https://doi.org/10.18280/ria.370207

[38] M. Bashiri and A. F. Geranmayeh, "Tuning the parameters of an artificial neural network using central composite design and genetic algorithm," *Sci. Iran.*, vol. 18, no. 6, pp. 1600–1608, 2011. https://doi.org/10.1016/j.scient.2011.08.031

[39] K. Suzuki, *Artificial Neural Networks: Architectures and Applications*. Rijeka, Croatia: InTech, 2013.

[40] F. Guo, J. Liu, C. Lv, and H. Yu, "A novel transformer-based network with attention mechanism for automatic pavement crack detection," *Constr. Build. Mater.*, vol. 391, p. 131852, 2023. https://doi.org/10.1016/j.conbuildmat.2023.131852

[41] Y. Zhang, Y. Zhu, H. Li, and J. Wang, "A hybrid optimization algorithm for multi-agent dynamic planning with guaranteed convergence in probability," *Neurocomputing*, vol. 592, p. 127764, 2024. https://doi.org/10.1016/j.neucom.2024.127764

[42] C. Torres-machi, A. Chamorro, C. Videla, E. Pellicer, and V. Yepes, "An iterative approach for the optimization of pavement maintenance management at the network level," *The Scientific World Journal*, vol. 2014, no. 1, p. 524329, 2014. https://doi.org/10.1155/2014/524329

[43] L. Kuruvachalil, F. Karim, A. R. Masoud, U. Hasan, L. Ali, F. B. Sulaiman, F. Alosaimi, and H. AlJassmi, "Advancing pavement management: A comprehensive review of smart models for better decisions," *Transp. Res. Interdiscip. Perspect.*, vol. 34, p. 101711, 2025. https://doi.org/10.1016/j.trip.2025.101711

[44] N. Yadav, A. Yadav, and M. Kumar, *An Introduction to Neural Network Methods for Differential Equations*. Warsaw: Springer, 2015.

[45] K. Naidu, M. S. Ali, A. H. A. Bakar, C. K. Tan, H. Arof, and H. Mokhlis, "Optimized artificial neural network to improve the accuracy of estimated fault impedances and distances for underground distribution system," *PLoS One*, vol. 15, no. 1, p. e0227494, 2020. https://doi.org/10.1371/journal.pone.0227494

[46] K. L. Priddy and P. E. Keller, *Artificial Neural Networks: An Introduction*. Bellingham, Washington: SPIE Press, 2005.

[47] A. Pollard, "What are neural networks," *Sens. Rev.*, vol. 10, no. 3, pp. 115–116, 1990. https://doi.org/10.1108/eb007822

[48] G. Montavon, G. B. Orr, and K. R. Mueller, Eds., *Neural Networks: Tricks of the Trade*. Berlin, Heidelberg: Springer, 2012.

[49] Y. Qin and C. Zheng, "A backpropagation neural network-based flexural-tensile strength prediction model for asphalt mixture in cold regions under cyclic thermal stress," *Math. Model. Eng. Probl.*, vol. 6, no. 3, pp. 433–436, 2019. https://doi.org/10.18280/mmep.060315

[50] H. Ceylan, C. W. Schwartz, S. Kim, and K. Gopalakrishnan, "Accuracy of predictive models for dynamic modulus of Hot-Mix Asphalt," *J. Mater. Civ. Eng.*, vol. 21, no. 6, pp. 286–293, 2009. https://doi.org/10.1061/(ASCE)0899-1561(2009)21:6(286)

[51] Z. Ye, Y. Xu, D. Veneziano, and X. Shi, "Evaluation of winter maintenance chemicals and crashes with an artificial neural network," *Transp. Res. Rec.*, vol. 2440, no. 1, pp. 43–50, 2014. https://doi.org/10.3141/2440-06

[52] A. Ilham, H. Hadiyanto, and C. E. Widodo, "Optimizing ANN-based Lyapunov stability for facial expression recognition as a base monitoring neurological disorders," *Int. J. Comput. Digit. Syst.*, vol. 14, no. 1, pp. 10 395–10 405, 2023. https://doi.org/10.12785/ijcds/1401109

[53] K. Adi, C. E. Widodo, A. P. Widodo, and F. Masykur, "Traffic violation detection system on two-wheel vehicles using convolutional neural network method," *TEM J.*, vol. 13, no. 1, pp. 531–536, 2024. https://doi.org/10.18421/TEM131

[54] P. W. Yunanto, R. Gernowo, and O. D. Nurhayati, "Prediction of traffic congestion based on time series dataset number of vehicles using neural network algorithm," vol. 2982, no. 1, p. 060007, 2024. https://doi.org/10.1063/5.0183639

[55] A. A. Ali, U. Heneash, A. Hussein, and S. Khan, "Application of artificial neural network technique for prediction of pavement roughness as a performance indicator," *J. King Saud Univ. Eng. Sci.*, vol. 36, no. 2, pp.

128–139, 2023. https://doi.org/10.1016/j.jksues.2023.01.001

[56] Y. I. Alatoom and T. I. Al-Suleiman, "Development of pavement roughness models using artificial neural network (ANN)," *Int. J. Pavement Eng.*, vol. 23, no. 13, pp. 4622–4637, 2021. https://doi.org/10.1080/10298436.2021.1968396

[57] M. B. Bayrak, E. Teomete, and M. Agarwal, "Use of artificial neural networks for predicting rigid pavement roughness," in *Midwest Transportation Consortium Fall Student Conference*, Ames, Iowa, 2004, pp. 1–18.

[58] K. Gurney, *An Introduction to Neural Networks*. London: Taylor & Francis e-Library, 2004.

[59] J. Yang, J. J. Lu, and M. Gunaratne, "Application of neural network models for forecasting of pavement crack index and pavement condition rating," 2003. https://fdotwww.blob.core.windows.net/sitefinity/docs/default-source/research/reports/fdot-bc353-13rpt.pdf

[60] W. Laosiritaworn and N. Chotchaithanakorn, "Artificial neural networks parameters optimization with design of experiments: An application in ferromagnetic materials modeling," *Chiang Mai J. Sci.*, vol. 36, no. 1, pp. 83–91, 2009.

[61] A. Sidess, A. Ravina, and E. Oged, "A model for predicting the deterioration of the pavement condition index," *Int. J. Pavement Eng.*, vol. 22, no. 13, pp. 1625–1636, 2021. https://doi.org/10.1080/10298436.2020.1714044

[62] A. A. Elhadidy, E. E. Elbeltagi, and M. A. Ammar, "Optimum analysis of pavement maintenance using multi-objective genetic algorithms," *HBRC J.*, vol. 11, no. 1, pp. 107–113, 2015. https://doi.org/10.1016/j.hbrcj.2014.02.008

[63] J. Santos, A. Ferreira, and G. Flintsch, "An adaptive hybrid genetic algorithm for pavement management," *Int. J. Pavement Eng.*, vol. 20, no. 3, pp. 266–286, 2019. https://doi.org/10.1080/10298436.2017.1293260

[64] K. Park, N. E. Thomas, and K. W. Lee, "Applicability of the international roughness index as a predictor of asphalt pavement condition," *J. Transp. Eng.*, vol. 133, no. 12, pp. 706–709, 2007. https://doi.org/10.1061/(ASCE)0733-947X(2007)133:12(706)

[65] S. S. Tehrani, L. C. Falls, and D. Mesher, "Road users' perception of roughness and the corresponding IRI threshold values," *Can. J. Civ. Eng.*, vol. 42, no. 4, pp. 233–240, 2015. https://doi.org/10.1139/cjce-2014-0344

[66] S. L. Chen, C. H. Lin, C. W. Tang, L. P. Chu, and C. K. Cheng, "Research on the international roughness index threshold of road rehabilitation in metropolitan areas: A case study in Taipei City," *Sustainability*, vol. 12, no. 24, p. 10536, 2020. https://doi.org/10.3390/su122410536

[67] Ministry of Public Works and Public Housing Directorate General of Highways, "Road pavement design manual (2017 revision)," 2017.

[68] Y. S. Chiou, M. C. Ho, P. Y. Song, J. D. Lin, S. H. Lu, and C. Y. Ke, "A study on the application of genetic algorithms to the optimization of road maintenance strategies," *Appl. Sci.*, vol. 15, no. 18, p. 10094, 2025. https://doi.org/10.3390/app151810094

[69] J. Xin, M. Akiyama, and D. M. Frangopol, "Sustainability-informed management optimization of asphalt pavement considering risk evaluated by multiple performance indicators using deep neural networks," *Reliab. Eng. Syst. Saf.*, vol. 238, p. 109448, 2023. https://doi.org/10.1016/j.ress.2023.109448

[70] K. S. Basnet, J. K. Shrestha, and R. N. Shrestha, "Pavement performance model for road maintenance and repair planning: A review of predictive techniques," *Digit. Transp. Saf.*, vol. 2, no. 4, pp. 253–267, 2023. https://doi.org/10.48130/dts-2023-0021

[71] A. Slowik and H. Kwasnicka, "Evolutionary algorithms and their applications to engineering problems," *Neural Comput. Appl.*, vol. 32, no. 16, pp. 12 363–12 379, 2020. https://doi.org/10.1007/s00521-020-04832-8

[72] C. S. K. Dash, A. K. Behera, S. Dehuri, and A. Ghosh, "An outliers detection and elimination framework in classification task of data mining," *Decis. Anal. J.*, vol. 6, p. 100164, 2023. https://doi.org/10.1016/j.dajour.2023.100164

[73] T. Tamagusko, M. G. Correia, and A. Ferreira, "Machine learning applications in road pavement management: A review, challenges and future directions," *Infrastructures*, vol. 9, no. 12, p. 213, 2024. https://doi.org/10.3390/infrastructures9120213

[74] M. Gharieb, T. Nishikawa, S. Nakamura, and K. Thepvongsa, "Modeling of pavement roughness utilizing artificial neural network approach for Laos national road network," *J. Civ. Eng. Manag.*, vol. 28, no. 4, pp. 261–277, 2022. https://doi.org/10.3846/jcem.2022.15851

[75] M. Ling, X. Luo, S. Hu, F. Gu, and R. L. Lytton, "Numerical modeling and artificial neural network for predicting J-Integral of top-down cracking in asphalt pavement," *Transp. Res. Rec.*, vol. 2631, no. January, pp. 83–95, 2017. https://doi.org/10.3141/2631-10

[76] H. Silaban, M. Zarlis, and S. Sawaluddin, "Analysis of accuracy and epoch on back-propagation BFGS Quasi-Newton," *J. Phys. Conf. Ser.*, vol. 930, no. 1, p. 012006, 2017. https://doi.org/10.1088/1742-6596/930/1/012006

[77] Z. Zhang, F. Feng, and T. Huang, "FNNS: An effective feedforward neural network scheme with random

weights for processing large-scale datasets," *Appl. Sci.*, vol. 12, no. 23, p. 12478, 2022. https://doi.org/10.3390/app122312478

[78] N. B. Shaik, S. R. Pedapati, S. A. A. Taqvi, A. R. Othman, and F. A. A. Dzubir, "A feed-forward back propagation neural network approach to predict the life condition of crude oil pipeline," *Processes*, vol. 8, no. 6, p. 661, 2020. https://doi.org/10.3390/PR8060661

[79] Y. Srinivas, A. S. Raj, D. H. Oliver, D. Muthuraj, and N. Chandrasekar, "A robust behavior of feed forward back propagation algorithm of artificial neural networks in the application of vertical electrical sounding data inversion," *Geosci. Front.*, vol. 3, no. 5, pp. 729–736, 2012. https://doi.org/10.1016/j.gsf.2012.02.003

[80] G. Fan, A. S. El-Shafay, S. A. Eftekhari, M. Hekmatifar, D. Toghraie, A. S. Mohammed, and A. Khan, "A well-trained artificial neural network (ANN) using the trainlm algorithm for predicting the rheological behavior of water–ethylene glycol/WO_3–MWCNTs nanofluid," *Int. Commun. Heat Mass Transf.*, vol. 131, p. 105857, 2022. https://doi.org/10.1016/j.icheatmasstransfer.2021.105857

[81] S. Inkoom, J. Sobanjo, A. Barbu, and X. Niu, "Pavement crack rating using machine learning frameworks: Partitioning, bootstrap forest, boosted trees, Naïve Bayes, and K-Nearest neighbors," *J. Transp. Eng. Part B Pavements*, vol. 145, no. 3, p. 04019031, 2019. https://doi.org/10.1061/jpeodx.0000126

[82] P. Marcelino, M. de Lurdes Antunes, E. Fortunato, and M. C. Gomes, "Machine learning approach for pavement performance prediction," *Int. J. Pavement Eng.*, vol. 22, no. 3, pp. 341–354, 2021. https://doi.org/10.1080/10298436.2019.1609673

[83] A. A. Ali, M. I. Esekbi, and M. M. Sreh, "Development of international roughness index from pavement distress using artificial neural networks (ANNs)," *Int. J. Adv. Eng. Bus. Sci.*, vol. 4, no. 1, pp. 179–192, 2023. https://doi.org/10.21608/ijaebs.2023.165192.1054

[84] S. Sultana, Y. Najjar, H. Yasarer, W. Uddin, and R. Barros, "International roughness index model for jointed reinforced concrete highway pavements: An artificial neural network application," in *Eleventh International Conference on the Bearing Capacity of Roads, Railways and Airfields*, 2022, pp. 246–255. https://doi.org/10.1201/9781003222910-25

[85] B. Rulian, Y. Hakan, S. Salma, and N. Yacoub, "Performance prediction model for jointed concrete pavements in Mississippi using machine learning," in *International Conference on Transportation and Development 2022*, 2022, pp. 153–164. https://doi.org/10.1061/9780784484319.015

[86] K. A. Abaza, "Simplified markovian-based pavement management model for sustainable long-term rehabilitation planning," *Road Mater. Pavement Des.*, vol. 24, no. 3, pp. 850–865, 2023. https://doi.org/10.1080/14680629.2022.2048055

[87] L. M. Pierce and G. McGovert, *Implementation of the AASHTO Mechanistic-Empirical Pavement Design Guide and Software*. Washington, DC: The National Academies Press, 2014.

[88] J. N. Meegoda and S. Gao, "Roughness progression model for asphalt pavements using long-term pavement performance data," *J. Transp. Eng.*, vol. 140, no. 8, p. 04014037, 2014. https://doi.org/10.1061/(ASCE)TE.1943-5436.0000682

[89] N. Kargah-Ostadi, S. M. Stoffels, and N. Tabatabaee, "Network-level pavement roughness prediction model for rehabilitation recommendations," *Transp. Res. Rec.*, vol. 2155, no. 1, pp. 124–133, 2010. https://doi.org/10.3141/2155-14

[90] D. T. Thube, "Highway development and management model (HDM-4): Calibration and adoption for low-volume roads in local conditions," *Int. J. Pavement Eng.*, vol. 14, no. 1, pp. 50–59, 2013. https://doi.org/10.1080/10298436.2011.606320

[91] C. S. Shahid, Z. A. Zainal, N. I. Md Yusoff, N. Mohammad, Z. H. Zamzuri, and I. Widyatmoko, "Stochastic-based pavement performance and deterioration models: A review of techniques and applications," *Alexandria Eng. J.*, vol. 120, pp. 420–437, 2025. https://doi.org/10.1016/j.aej.2025.02.033